CTP:Phosphocholine Cytidylyltransferase Activation by Oxidized Phosphatidylcholines Correlates with a Decrease in Lipid Order: A ^{2}H NMR Analysis†

Adrienne E. Drobnies,‡ Bryan van der Ende,§,|| Jenifer L. Thewalt,‡,§ and Rosemary B. Cornell*,‡

Institute of Molecular Biology and Biochemistry and Department of Physics, Simon Fraser University, Burnaby, British Columbia, Canada, V5A 1S6

Received July 8, 1999; Revised Manuscript Received September 17, 1999

ABSTRACT: The enzyme CTP:phosphocholine cytidylyltransferase (CT) binds reversibly to membranes and is active only in its membrane-bound form. Membrane lipid composition influences the equilibrium between its soluble and membrane-bound forms. Whereas the enzyme is not activated by phosphatidylcholine (PC) vesicles, it is activated by PC vesicles that have been oxidized with $HClO_4$ [Drobnies, A. E., et al. (1998) *Biochim. Biophys. Acta 1393*, 90−98]. Here we explore the mechanism of activation of CT by a PC oxidized with lipoxidase. Multilamellar vesicles (MLVs) containing ≥5 mol % oxidized 1-palmitoyl-2-arachidonoylPC (PAPC) progressively activated the enzyme, which was fully activated by 25 mol % oxidized PC. The effect of oxidized PAPC on lipid order was investigated by ^{2}H NMR, using MLVs containing PAPC perdeuterated on the palmitoyl chain. Spectral depaking generated order parameter profiles along the *sn*-1 chain. The average order parameter (S_{CD}) in the plateau region at 37 °C decreased from 0.18 to 0.15 with increasing percent of oxidized PAPC (0−25%). The change in S_{CD} was even greater near the end of the palmitoyl chain. CT activation was inversely related to lipid order. The major component of the lipoxidase-oxidized PAPC was purified and characterized by mass spectrometry and NMR. This component, 1-palmitoyl-2-(11,15-dihydroxy)eicosatrienoylPC (dihydroxyPAPC), incorporated into PAPC MLVs, also stimulated CT activity and reduced the lipid order parameter. Both effects were reversed by egg sphingomyelin. We propose that CT activation by oxidized PAPC is mediated by effects on lipid packing perturbations. This is the first study to report the effects of a purified oxidized PC on the orientational order along the acyl chain and to correlate the lipid disordering of the oxidized PC with the activation of a membrane-associated regulatory enzyme.

Reactive oxygen species (ROS) are emerging as important mediators of cell signaling in mitogenesis and programmed cell death (*1*−*3*). Their molecular targets and mechanisms of action are poorly defined, and may be diverse. One of the prominent targets for ROS are the polyunsaturated phospholipids found in cell membranes (*4*). These oxidized lipids may participate in the signal transduction pathways downstream of ROS production via direct modulation of the activity of membrane-associated enzymes. There are a few examples of membrane- or lipoprotein-associated enzymes whose activities are influenced by oxidized lipids; however, the underlying mechanisms are not clear. For example, the enzyme 5-lipoxygenase was activated allosterically by a hydroperoxy-fatty acid in vitro (*5*). Lipid hydroperoxides inactivated lecithin:cholesterol acyltransferase, perhaps by oxidizing the enzyme's free cysteines (*6*, *7*). The intracellular phospholipase $cPLA_2$[1] was more active toward its lipid substrate if the lipid vesicles contained hydroperoxylPC (*8*). Oxidized PC is a preferred substrate for secreted forms of PLA_2 due to improved access of the enzyme to the *sn*-2 ester bond (*9*). In addition, phospholipase D and protein kinase C are activated in cells stimulated with oxidized LDL, although there is no evidence implicating direct modulation by oxidized lipid components (*10*, *11*).

Recently, we showed that hypochlorite-oxidized PCs activate CTP:phosphocholine cytidylyltransferase (CT), a key regulatory enzyme in PC synthesis (*12*). CT activation by

† This work has been funded by the Heart and Stroke Foundation of Canada.

* Corresponding author. Fax: +1 604 291 5583. E-mail: cornell@sfu.ca.

‡ Institute of Molecular Biology and Biochemistry.

§ Department of Physics.

|| Current address: Department of Physics, University of Guelph, Guelph, ON, Canada, N1G 2W1.

[1] Abbreviations: PC, phosphatidylcholine; CT, CTP:phosphocholine cytidylyltransferase; SUVs, small unilamellar vesicles; MLVs, multilamellar vesicles; PAPC, 1-palmitoyl-2-arachidonoylphosphatidylcholine; PL_3PC, 1-palmitoyl-2-linolenoylphosphatidylcholine; PL_2PC, 1-palmitoyl-2-linoleoylphosphatidylcholine; POPC, 1-palmitoyl-2-oleoylphosphatidylcholine; DL_2PC, dilinoleoylphosphatidylcholine; 31d-PAPC, PAPC perdeuterated on the palmitoyl chain; SM, egg sphingomyelin; PC/O (1:1), egg PC/oleic acid (1:1); LOX-PAPC, lipoxidase-oxidized PAPC; dihydroxyPAPC, 1-palmitoyl-2-(11,15-dihydroxy)-eicosatrienoylphosphatidylcholine; 15-hydroxyPAPC, 1-palmitoyl-2-(15-hydroxy)eicosatetraenoylPC; ESR, electron spin resonance; AFD, angle-resolved fluorescence depolarization; MS, mass spectrometry; PLA_2, phospholipase A_2; BHT, butylated hydroxytoluene; ^{3}H-DPPC, [*methyl*-^{3}H]choline (^{3}H-choline); COSY, correlation spectroscopy; TOCSY, total correlation spectroscopy.

10.1021/bi991573v CCC: $18.00
Published on Web 11/04/1999

oxidized membrane PCs may contribute, in addition to PLA_2 (*9*), to the repair of ROS-damaged membranes.

CT is an amphitropic enzyme (*13*), and the interaction of CT with membrane lipids is required for its activation. Membrane binding and activation is inhibited by the pathway end-product, PC, and is promoted by a number of lipids with diverse structures. Fatty acids and anionic phospholipids constitute one class of lipids that promote membrane binding and enzyme activation (*14*−*20*). Neutral lipids with small polar headgroups, such as diacylglycerol, constitute a second class (*16*−*20*). Unsaturated phosphatidylethanolamine constitutes a third (*21, 22*). The anionic lipids promote electrostatic localization of CT to the membrane surface. The electrostatic binding is insufficient for activation; rather, activation requires intercalation of the hydrophobic face of the amphipathic helical membrane binding domain into the fatty acyl core (*13, 23, 24*). Thus, lipids which facilitate the insertion process will function as enzyme activators. One potentially unifying feature of all types of lipid activators may be their ability to disrupt the packing of lipid bilayers. There are many observations which support this proposal: (i) CT activation by lipid vesicles of the same composition is sensitive to the geometric curvature; i.e., it shows preference for highly curved SUVs over planar MLVs (*17*). (ii) CT is sensitive to the phase of the lipids, and is anomalously activated at the gel-to-liquid crystalline phase transition (*17*). (iii) Binding of peptides corresponding to the membrane binding domain to phospholipid monolayers is sensitive to the initial surface pressure, and the selectivity for acidic lipids vs PC disappears at low surface pressure, suggesting that high lipid packing density is a barrier toward CT intercalation (*24*).

Oxidized phospholipids may facilitate the CT insertion/activation process by disordering the membrane. Three previous reports suggest that oxidation of phospholipids perturbs lipid packing and bilayer order. Oxidation from the reaction of soybean 15-lipoxidase on PL_2PC and DL_2PC decreased membrane order as assessed by electron spin resonance (ESR) with a doxylcholestane probe, and angle-resolved fluorescence depolarization (*25*). The disordering effects were greater in DL_2PC than in PL_2PC, as determined by the AFD technique. Order parameters decreased with increasing mole percent of 1-palmitoyl-2-(15-hydroxy)-eicosatetraenoylPC (15-hydroxyPC) in liposomes composed of PAPC plus cholesterol, as monitored by ESR with a doxylPC probe (*26*). Surface pressure changes of spread monolayers demonstrated that air-oxidized PL_2PC hydroperoxides and hydroxides occupy a 50% increased molecular surface area (*9*).

In this work, we have examined the effects of oxidized PCs on bilayer order using ^2H NMR and have correlated the changes in membrane order with ability to activate CT. In addition to its nonperturbing nature, this method allows for determination of order parameter as a function of carbon number along the deuterated chain. PC oxidation was catalyzed by soybean 15-lipoxidase (*25, 27*). The primary product is a hydroperoxyl addition at the 13-carbon position on the linoleoyl chain and at the 15-carbon position on the arachidonoyl chain (*28*). The expected reaction with PAPC is depicted in Figure 1, as is the rearrangement that is presumed to occur in order to produce the dihydroxyPAPC, which we have purified as the major component of the

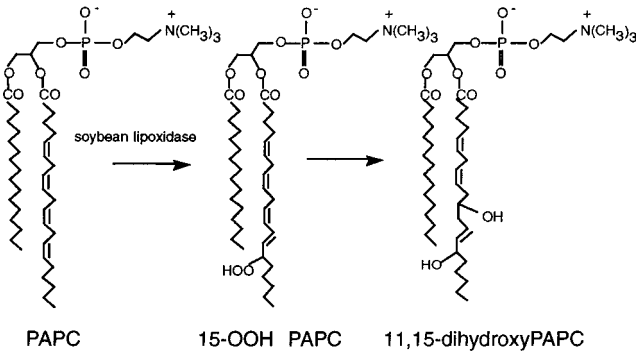

FIGURE 1: Reaction of PAPC with soybean lipoxidase. The primary product is the 15-hydroperoxy derivative on the arachidonoyl chain. The major product isolated from the reaction mixture is 11,15-dihydroxyPAPC.

reaction mixture. The oxidized PAPC was tested as a component of MLVs containing 31d-PAPC for effects on the NMR spectra of the ^2H-labeled lipid and CT activity. CT activity was increased, and the molecular order was correspondingly decreased by increasing mole percent oxidized PAPC. Both effects of the oxidized PC were reversed by egg sphingomyelin. Sphingomyelin has been shown to increase membrane order (*29*). We therefore propose that CT activation by oxidized phospholipids is mediated by their membrane disordering effects.

EXPERIMENTAL PROCEDURES

Materials. Phospholipids were purchased from Avanti (Birmingham, AL) and stored as chloroform or chloroform/methanol solutions under argon at −20 °C. Concentrations were verified by phosphorus assay (*30*). Soybean lipoxidase type IV, butylated hydroxytoluene (BHT), deuterium-depleted water, choline kinase, and CTP were purchased from Sigma. Analytical (0.46 cm i.d. × 25 cm) and semipreparative (1 cm × 25 cm) ODS columns (5 μm particle size) were purchased from Beckman. HPLC-grade methanol and other solvents were from Mallinckrodt. [*methyl*-^3H]-Dipalmitoylphosphatidylcholine (^3H-DPPC) was from Amersham, and [*methyl*-^3H]-choline (^3H-choline) was from New England Nuclear. Silica gel H self-char plates containing 5% ammonium sulfate (20 × 20 cm) were from Analtech. Lipid hydroperoxide assay kit was from Cayman Chemical (Ann Arbor, MI).

Lipoxidase Reaction. PAPC (75−150 μmol dried from chloroform solution) was suspended in 0.2 M borate, pH 9, 10 mM deoxycholate to a final concentration of 1 mM. Soybean lipoxidase (type IV) [(1.9−3.8) × 10^7 units] was reacted with the lipid with gentle shaking, open to air, for 90 min at 30 °C (*27*). Reactions with PL_3PC, PL_2PC, and POPC were done using similar conditions but smaller quantities of lipid (1 μmol) and lipoxidase (2.5 × 10^5 units).

Purification and Characterization of Reaction Products. At the end of the reaction, the mixture was dialyzed extensively at room temperature for 4 days with changes every 4−8 h against 0.2 M NaCl, 10 mM Tris, pH 8, 0.5 mM EDTA, 0.5 mM BHT, using dialysis tubing with MWCO = 12 000−14 000, to remove deoxycholate. The last change of dialysis buffer omitted the NaCl. The complete removal of deoxycholate from the preparation was confirmed by TLC on an aliquot of the dialysate. The final dialysate

was extracted into chloroform (*31*) and concentrated by rotary evaporation. A phosphorus analysis (*30*) determined the final concentration of lipid. The TLC system to separate oxidized from parent PCs employed Silica gel H, impregnated with ammonium sulfate (self-char). The solvent system was chloroform/methanol/water (65:24:4) (*27*). Lipids were visualized by heating the plates in an oven at 180 °C for 20 min.

Conjugated Diene Analysis. The dialyzed, extracted reaction product was dried and redissolved in 1 mL of cyclohexane. The UV spectrum of an aliquot containing 5 nmol of lipid was measured from 205 to 305 nm. The ratio of absorbance at 235 nm to that at 205 nm was used as an index of conjugated diene formation (*32*).

High Performance Liquid Chromatography. Lipoxidase-treated PCs (150 nmol) were dissolved in 50 μL of methanol for injection onto an analytical (0.46 × 25 cm) ODS column. Lipid species were eluted with 100% methanol at a flow rate of 1 mL/min (*25*). Absorbance was recorded at 200, 234, and 275 nm. The major peak, which eluted at 7.4 min, was purified from a 150 μmol scale oxidized PAPC preparation by repetitive injections onto a semipreparative (1 × 25 cm) ODS column (Figure 2A). The column was eluted with 100% methanol at 4 mL/min. The peak eluting between 7.0 and 7.9 min (Figure 2B) was collected on ice and stored under argon. These purified fractions were pooled and dried by rotary evaporation. After dissolution into methanol, a sample was then reinjected onto the semipreparative column, to assess its purity. The concentration of the pooled purified fraction was determined by phosphorus analysis (*30*).

Mass Spectrometry. The molecular weight of the purified product was determined by electrospray mass spectrometry in the positive mode, using a Quattro I (Micromass) system. Two micrograms of lipid in methanol was analyzed by direct liquid injection in the presence of 0.1% formic acid at a flow rate of 50 mL/min. Mass was scanned over the range 500−900 atomic mass units.

^{1}H and ^{13}C NMR. The purified component from PAPC oxidation (3.4 mg dissolved in $CDCl_3$ or benzene-d_6) was analyzed by ^{1}H and ^{13}C NMR, using a Bruker AMX400 spectrometer operating at ambient temperature. 2-D COSY, TOCSY, and heteronuclear correlation spectra were obtained using standard conditions (*33*). ^{13}C 1-D and ^{1}H/^{13}C 2-D correlation spectra were obtained from the phospholipid in deuterated chloroform solution only.

Sample Preparation for ^{2}H NMR. NMR samples consisted of 22 mg of 31d-PAPC plus 0−7 mg of the lipoxidase-oxidized PAPC (0−25 mol % LOX-PAPC) or 0, 3.2, or 4.9 mg of dihydroxyPAPC (0, 12, 20 mol % diOHPAPC). In the experiments to study the effect of sphingomyelin, NMR samples consisted of 17.8 mg of 31d-PAPC plus 6.6 mg of egg SM (70 mol % 31d-PAPC/30 mol % SM); or 11 mg of 31d-PAPC, 4.4 mg of diOHPAPC, and 5.8 mg of egg SM (50 mol % 31d-PAPC/30 mol % SM/20 mol % diOHPAPC); or 11 mg of 31d-PAPC and 2.7 mg of diOHPAPC (80 mol % 31d-PAPC/20 mol % diOHPAPC). Lipids were mixed as $CHCl_3$ solutions and then dried under nitrogen and vacuum. MLV suspensions (28−60 mM) were prepared by vigorous vortexing of lipids in 0.6 mL of ^{2}H-depleted water containing 20 mM Tris, pH 7.4, 0.5 mM EDTA. The integrity of the MLVs was assessed by centrifugation of [^{3}H]-DPPC trace-labeled MLVs at 15 000 rpm for 20 min. The average recovery of tracer in the pellet was 90% for 0−50 mol % oxidized lipid. The mole percent of oxidized product in each sample was verified by HPLC before and after each NMR measurement. Negligible changes in the percent oxidation occurred during the NMR analysis.

^{2}H NMR Methods. Spectra were obtained using the quadrupolar echo technique (*34*) with a custom-built spectrometer (*35, 36*) operating at 46.2 MHz. The typical spectrum resulted from 24 000−48 000 scans of the two-pulse sequence with a 90° pulse length of 3.75−3.95 μs, an interpulse spacing of 40 μs, and a dwell time of 2 μs. The delay between acquisitions was 300 ms, and 4K data points per acquisition were collected in quadrature with 8-cyclops phase cycling. Order parameter profiles (the carbon−deuterium orientational order parameter, S_{CD}, vs position along the deuterated palmitoyl chain) were calculated from depaked spectra (*37*) using the method outlined by Lafleur et al. (*38*). Those spectra featuring an intense sharp central absorption peak, referred to as the isotropic component, were treated as follows in order to calculate order parameter profiles from the underlying Pake doublet spectra. Beginning at approximately 400 μs after the top of the quadrupolar echo, the free induction decays (FIDs) were fit to a sum of two exponentials. This fit was extrapolated back to the top of the echo and subtracted from the FID prior to Fourier transformation and depaking.

Miscellaneous Assays. CT activity assay was carried out as described previously (*12*). The concentration of MLVs in the assay was 1 mM. *The lipid hydroperoxide assay* (Cayman Chemical) measured the reaction of ferrous ion (Fe^{2+}) with lipid hydroperoxide to produce ferric ion (Fe^{3+}), which forms a complex with thiocyanate ion (SCN^-). The absorbance of the complex at 500 nm was used to determine the amount of lipid hydroperoxide present. The standard for the assay was 13-hydroperoxyoctadecadienoic acid.

RESULTS

Comparison of CT Activation by Lipoxidase Products of PAPC, PL$_3$PC, PL$_2$PC, and POPC. All PC species were subjected to lipoxidase-catalyzed oxidation and dialysis as described under Experimental Procedures. The degree of oxidation was assessed by the formation of conjugated dienes. According to this measure of oxidation, the degree of oxidation was $PL_2PC > PL_3PC > PAPC > POPC$. The absorbance ratios (235/205 nm) were 0.056, 0.022, 0.093, and 0.023 for the unoxidized PAPC, PL_3PC, PL_2PC, and POPC, respectively. For the oxidized lipids, absorbance ratios were 0.366, 0.645, 1.05, and 0.024 for PAPC, PL_3PC, PL_2-PC, and POPC, respectively. Figure 3 shows the effects of oxidized PC species on CT activity. Neither oxidized PL_2-PC nor POPC-activated CT compared to the unoxidized control. Oxidation of PL_3PC activated CT 1.6-fold; oxidation of PAPC activated CT 2.1-fold, which is the same degree of activation obtained with egg PC/oleic acid (1/1) sonicated vesicles, i.e., maximal activity (*15, 17*). These results are consistent with our earlier observations using hypochlorite-oxidized phospholipids (*12*). Since oxidized PAPC had the greatest effect on CT activity, PAPC was used in the remainder of this study.

Soybean Lipoxidase Catalyzed Oxidation of PAPC, and Purification and Characterization of the Major Product. The

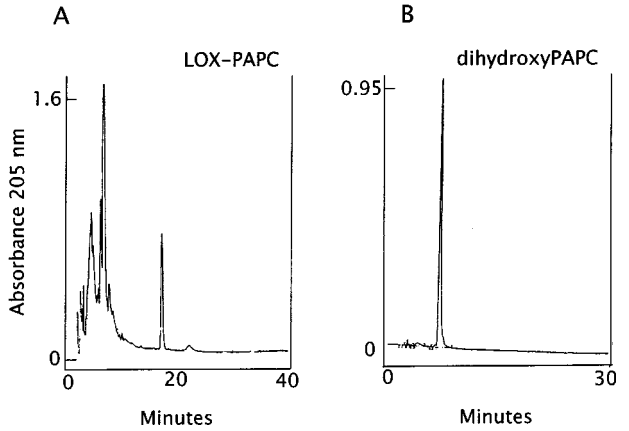

FIGURE 2: HPLC analysis and purification of reaction products of 1.9×10^7 units of soybean lipoxidase with 75 μmol of PAPC for 90 min at 30 °C. Chromatography was carried out as described under Experimental Procedures on a semipreparative ODS column, and absorbance was monitored at 205 nm. (A) LOX-PAPC (2 mg) injected in 60 μL of methanol. The peak corresponding to unoxidized PAPC is at 17.4 min (8.5% total area), and oxidized peaks are before 10 min. (B) The peak between 7 and 8 min, dihydroxyPAPC (0.5 mg), in 30 μL of methanol was reinjected onto the column after purification from the mixture shown in (A).

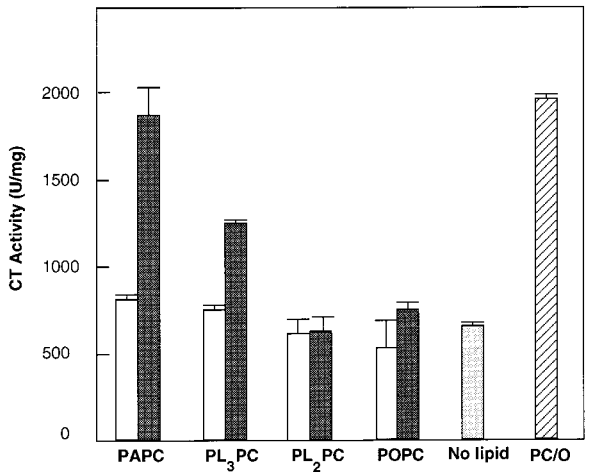

FIGURE 3: Activation of CT by lipoxidase-oxidized phospholipids. The activity of CT was measured in duplicate assays in the presence of 1 mM MLVs composed of these lipids as described under Experimental Procedures. Open bars represent CT activity for unoxidized controls, and shaded bars represent values for oxidized phospholipids. Values for the PL_2PC control and PC/O are from separate assays and were normalized to the no-lipid values presented in this figure.

mixture of PAPC oxidation products (LOX-PAPC), generated from the reaction catalyzed by soybean lipoxidase, was analyzed by TLC and HPLC. The thin-layer chromatogram of the products of the lipoxidase reaction showed PAPC at $R_f = 0.5$ and up to four more slowly migrating species. Deoxycholate ($R_f = 0.85$) was not detected by TLC of 100 nmol of the oxidized, dialyzed sample. The amount of detergent or lipid that can be observed by the TLC procedure was approximately 5 nmol. Therefore, the reaction mixture after dialysis is estimated to contain less than 5 mol % deoxycholate. A faint spot for arachidonic acid ($R_f = 0.95$) was present in the chromatogram, and was estimated by densitometry to be approximately 6% of the total lipid present in the oxidized lipid. Conjugated diene formation, a measure of the degree of oxidation, was analyzed by the ratio of absorbance at 235/205 nm. This ratio was 0.61 for the oxidized sample, and 0.056 for the unoxidized control. The HPLC profile of products from a lipoxidase reaction is shown in Figure 2A. The HPLC profile for the unfractionated mixture of oxidized products consisted of a number of peaks which eluted between 2.5 and 11 min. The unreacted PAPC eluted at 17.4 min and constituted less than 9% of the total integrated intensity from the HPLC profile.

The major oxidized component at 7.4 min, which contained 27% of the total integrated peak intensity, was purified further by HPLC. The purified product eluted as a single peak that corresponded to 95% of the total integrated peak intensity (Figure 2B). A molecular weight of 816 was obtained by electrospray mass spectrometry, consistent with the addition of two oxygens to PAPC. A test for hydroperoxides was performed on 2.5, 12.5, and 25 nmol of the oxidized PAPC, which detects hydroperoxides in the range of 0−5 nmol. Results on all samples indicated the presence of <0.5 nmol of lipid hydroperoxide. We concluded that the phospholipid was not a hydroperoxide.

^{13}C NMR spectroscopy demonstrated the loss of one double bond. COSY and TOCSY spectra distinguished headgroup, *sn*-1, and *sn*-2 chain resonances. From these spectra, there was no ambiguity in proton assignment within the unsaturated chain from positions 2−6 and positions 16−20. C5 and C6 were olefinic. Of the remaining signals, two of a number of overlapping proton signals had J_{CH} values of 178 Hz (2.77 ppm ^1H/61.7 ppm ^{13}C) and 175 Hz (2.81 ppm ^1H/57.8 ppm ^{13}C). These were assigned to carbons bearing hydroxyl groups. The remaining coupling constants were on the order of 125 Hz (aliphatic chain), 146 Hz (headgroup and CH_2 groups adjacent to olefinic residues), and 158 Hz (olefinic). An attempt was made to unambiguously assign signals from positions 7 through 15 by changing the solvent from chloroform to benzene. Changing the solvent to benzene moved signals significantly but did not resolve the crucial overlapping signals at 2.9 ppm (hydroxy) and 5.4 ppm (olefinic) in the ^1H spectra. The NMR spectra could not therefore be used to unambiguously assign the hydroxyl substitution positions. There were three possible sequences that fit the data. The substitution pattern that best fit the data was the hydroxyl substitutions on the 11 and 15 carbons of the arachidonoyl chain. A second possibility was substitution at the 8 and 15 carbons, and the poorest fit was associated with substitution at the 7 and 8 carbons. Based on the preference for attack at C15 in lipoxidase-catalyzed oxidations, and the chemistry of the oxidative electronic arrangements, we propose 11,15-dihydroxyPAPC (Figure 1) as the purified component.

Effect of LOX-PAPC on Lipid Order. To assess the effects of oxidized PAPC on the lipid packing disorder, we obtained ^2H NMR spectra of 31d-PAPC mixed with various mole fractions of oxidized PAPC. ^2H NMR quadrupolar splittings observed in liquid crystalline membranes are directly proportional to orientational order, i.e., the time average of the C−D bond orientation with respect to the bilayer normal (*39*).

The ^2H NMR spectra of 31d-PAPC membranes containing 0, 10, and 15 mol %[2] LOX-PAPC are shown in Figure 4.

[2] Stock 31d-PAPC contains 3−5% nonspecific oxidation products (by HPLC), which were present in all samples.

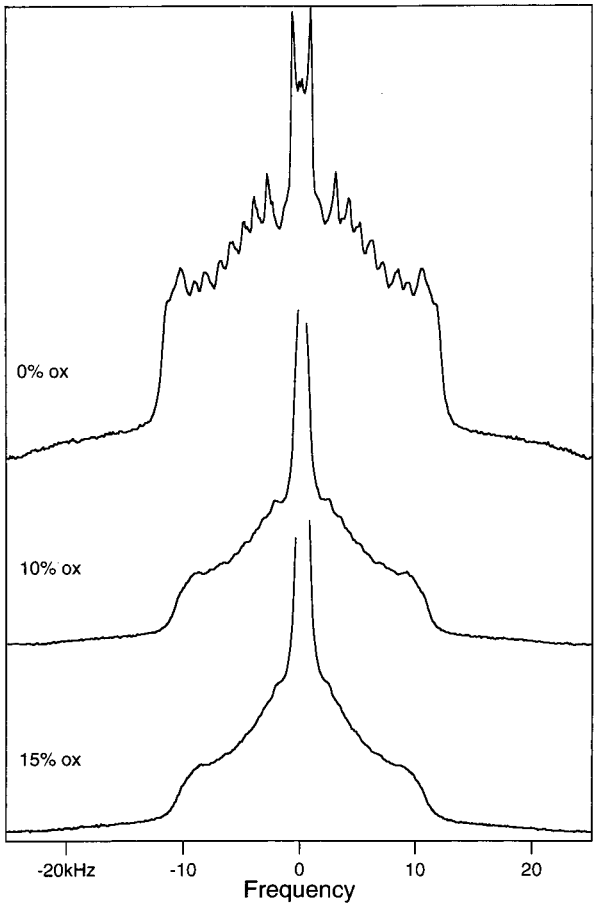

FIGURE 4: ^{2}H NMR spectra at 37 °C of 31d-PAPC containing the following mol % LOX-PAPC: 0 (upper), 10 (middle), and 15 (lower). Central points of the spectrum corresponding to the isotropic component have been omitted for the 10 and 15 mol % spectra.

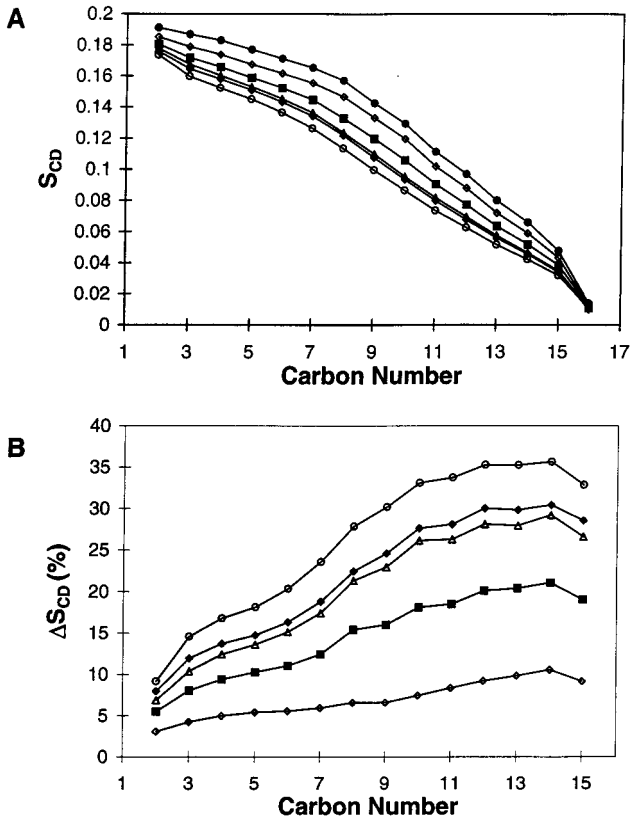

FIGURE 5: (A) Order parameter (S_{CD}) at 37 °C for each carbon on the labeled palmitoyl chain of 31d-PAPC in the presence of increasing mol % LOX PAPC: 0 (●), 5 (◇), 10 (■), 15 (△), 20 (◆), 25 (○). (B) Percent change in the S_{CD} as a function of chain position in 31d-PAPC with increasing mol % LOX-PAPC, using the 0 mol % LOX-PAPC as the reference sample. Symbols are the same as in (A).

At the lowest proportion of LOX-PAPC, the individual Pake doublets making up the spectrum are well resolved. The order parameter profile (the absolute value of the order parameter, S_{CD}, vs carbon number for each carbon along the palmitoyl chain) was calculated assuming a monotonic decrease in the quadrupolar splitting from C-2 to C-16 (Figure 5A). At higher mole fractions of oxidized lipids, the spectrum became blurred, presumably due to membrane heterogeneity. Although the resolution was less for the individual Pake doublets in these spectra, the depaking procedure permitted the calculation of order parameter profiles. (T_{2e}, the relaxation time characterizing the decay of the quadrupolar echo height as a function of pulse spacing, was shorter in the presence of oxidized lipids. There was no evidence of spectral distortion due to orientation-dependent T_{2e}, however.) The reduction in S_{CD} for all positions along the deuterated chain as a function of the membrane's LOX-PAPC content, in comparison with the 0 mol % LOX-PAPC membrane, is shown in Figure 5B.

An increase in a temperature-dependent isotropic component was observed with increasing mole percent oxidation product (Figure 4). The integrated intensity of this component increased upon heating and decreased again upon cooling. The magnitude of the isotropic component varied between different preparations of oxidized lipid. For example, in the preparation used to prepare membranes whose spectra are shown in Figure 4, the isotropic component constituted 10% of the total intensity of the spectrum of the membrane containing 15% LOX-PAPC, but constituted less than 3% in a subsequent preparation. Despite the variation in isotropic component, both preparations of LOX-PAPC activated CT nearly equally.

Relationship between CT Activity and Molecular Order. Figure 6 compares the effects of LOX-PAPC on the activation of CT with its effects on the lipid order parameter in the plateau region of the spectra (S_{CD} associated with carbons 2−7). The comparison to the proximal portion of the acyl chain was made since it is into this region that CT inserts (*40*). Lipid order and CT activity were inversely proportional.

Effect of DihydroxyPAPC on Lipid Order. The ^{2}H spectra of 31d-PAPC membranes containing 0, 12, and 20 mol % dihydroxyPAPC are shown in Figure 7. The resolution of individual Pake doublets was improved and the isotropic component was diminished compared to the spectra for the unfractionated LOX-PAPC (Figure 4). The order parameters derived from the depaked spectra and the percent change in order parameter (compared to the membrane containing 0 mol % dihydroxyPAPC) at each carbon are shown in Figure 8A and 8B.

From these results, it is apparent that order decreases at every carbon on the deuterated palmitoyl chain of PAPC with increasing percent oxidized component, both in the samples containing the unfractionated oxidized mixture and in those containing the purified dihydroxyPAPC. The greatest frac-

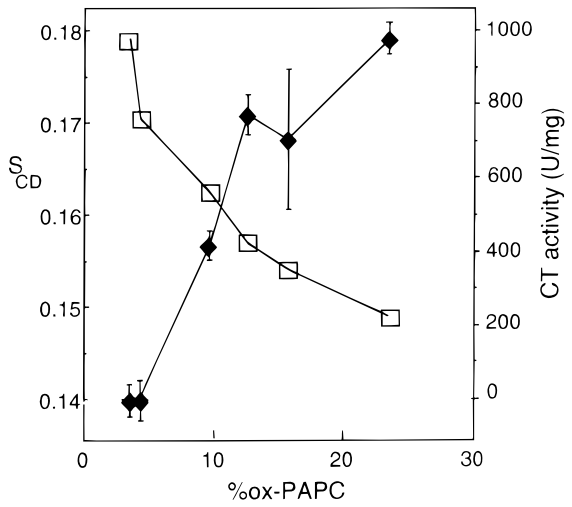

FIGURE 6: CT activity is inversely related to the order parameter. The same liposomes were used for CT activity and ^{2}H NMR. CT activity values (◆) were the average of duplicate determinations, and were corrected for activity in the absence of lipid (660 ± 21 units/mg). Average values (□) of the S_{CD} in the plateau region are for carbons 2−7 on the palmitoyl chain. Values for ox-PAPC are the average of the integrated intensity for all the oxidized peaks in the HPLC before and after the NMR measurements.

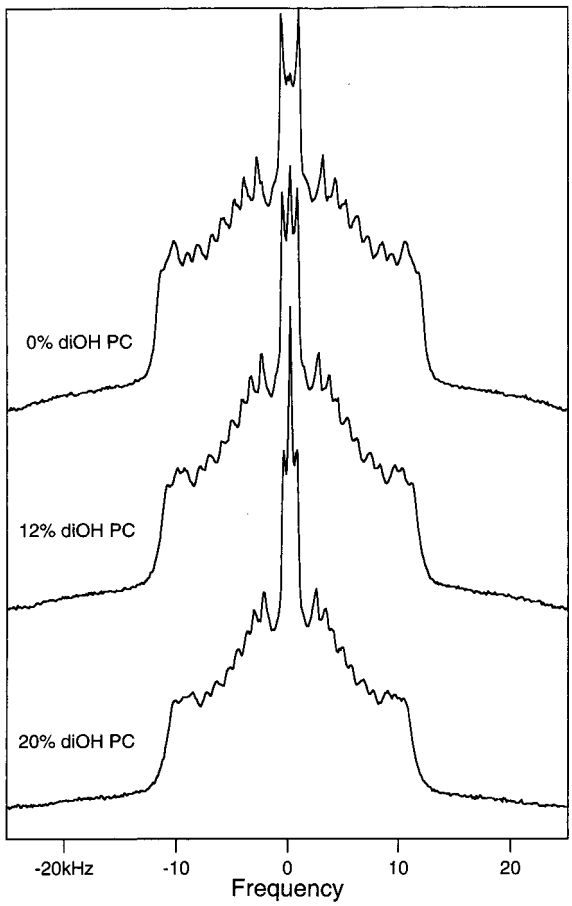

FIGURE 7: ^{2}H NMR spectra at 37 °C of 31d-PAPC containing dihydroxyPAPC at the following mol %: 0 (upper), 12 (middle), 20 (lower).

tional changes in molecular order associated with the oxidized PC are between carbons 10 and 15. The largest increment in the ΔS_{CD} is carbons 7−10.

Comparison of the Effects of DihydroxyPAPC and LOX-PAPC on CT Activity. The effects of dihydroxyPAPC and

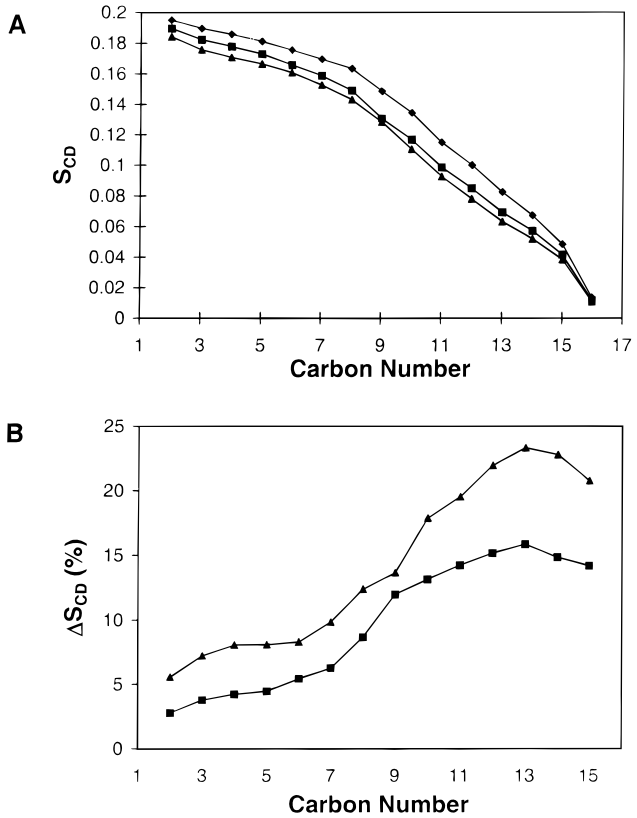

FIGURE 8: (A) Order parameter (S_{CD}) at 37 °C for each carbon on the labeled palmitoyl chain of 31d-PAPC in the presence of increasing mol % dihydroxyPAPC: 0 (◆), 12 (■), 18 (▲). (B) Percent change in the S_{CD} observed as a function of chain position in 31d-PAPC with increasing mol % dihydroxyPAPC, using the 0% dihydroxyPAPC as the reference sample. Symbols are the same as in (A).

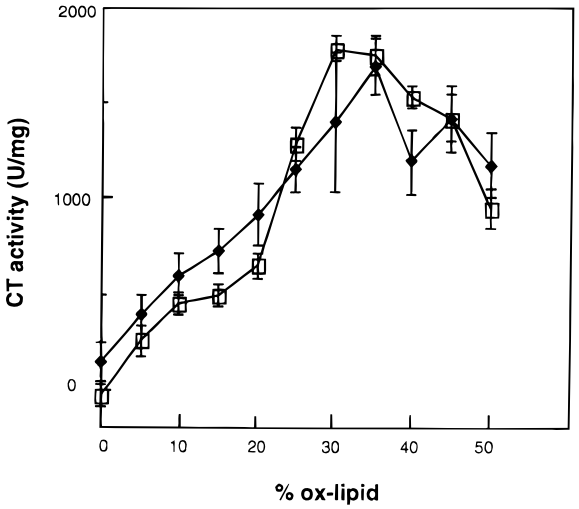

FIGURE 9: CT activation by dihydroxyPAPC and LOX-PAPC. The % oxidized lipid refers to total oxidized PC species generated by LOX (◆) or the mol % dihydroxyPC (□). The balance of the lipid in the MLVs was unoxidized PAPC. The activity values represent the average of triplicate determinations and are corrected for the activity in the absence of lipid (1516 ± 34 units/mg).

the unfractionated LOX-PAPC were also compared in simultaneous activity assays (Figure 9). The activation of CT by dihydroxyPAPC was nearly identical to that observed for the unfractionated mixture, suggesting that the compound we isolated is one of several oxidized species in LOX-PAPC that activates CT. In the oxidized mixture, 11,15-dihyroxyPC

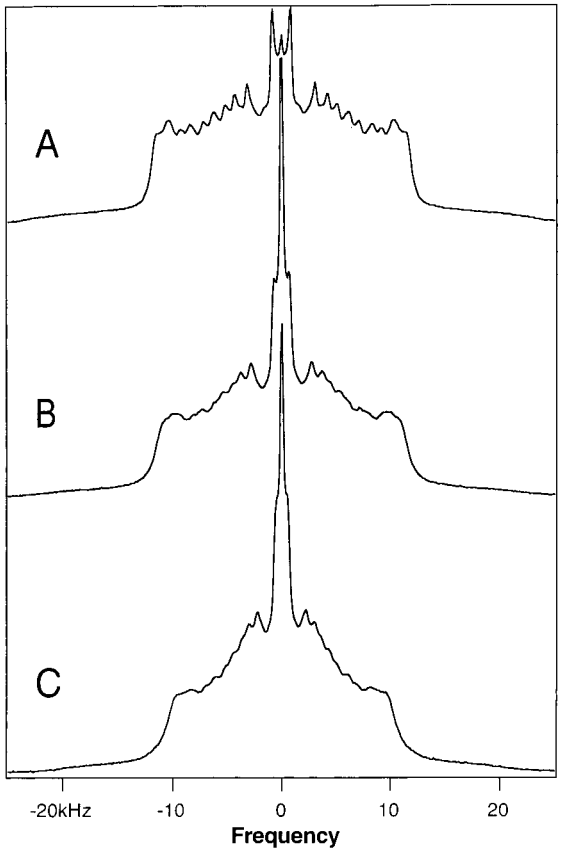

FIGURE 10: ^{2}H NMR spectra at 37 °C of MLVs composed of (A) 70 mol % 31d-PAPC/30 mol % SM, (B) 50 mol % 31-d PAPC/30 mol % SM/20 mol % diOHPAPC, and (C) 80 mol % 31d-PAPC/20 mol % diOHPAPC.

is only 27% of the total oxidized PC species, yet 25 mol % of this mixture activates CT to the same extent as 25 mol % of the purified component.

Effect of Sphingomyelin on Bilayer Order of PAPC and PAPC/DihydroxyPAPC Mixtures. ^{2}H NMR spectra of 31d-PAPC containing egg sphingomyelin and/or dihydroxyPAPC are shown in Figure 10. In egg sphingomyelin, the fatty acid content is 77.7% palmitoyl (16:0). In these spectra, the largest quadrupolar splittings were observed for 31d-PAPC/SM (70/30) and the smallest for 31d-PAPC/dihyroxyPAPC (80/20). Intermediate splittings were observed for 31d-PAPC/SM/dihydroxyPAPC (50/30/20). Order parameter profiles for each of these spectra are shown in Figure 11, along with the profile for 31-d PAPC. It is apparent that 30% sphingomyelin completely opposed the disordering effect of 20% dihydroxyPAPC all along the palmitoyl chain.

Effect of Sphingomyelin on Activation of CT by DihydroxyPAPC. The effects of sphingomyelin on CT activity are shown in Figure 12. Sphingomyelin caused a statistically significant inhibition of CT activity when present as a component of PAPC/dihyroxyPAPC or PAPC MLVs. When SM was varied from 0 to 30 mol % in PAPC MLVs containing 20 or 30 mol % dihydroxyPAPC, a progressive reversal of the activation of CT by dihydroxyPAPC was also seen in two separate experiments (data not shown). Furthermore, when the mole ratio of SM was varied in PAPC MLVs *without* dihyroxyPAPC, an inhibitory trend was also seen. These results are consistent with the activity results presented in Figure 12. Figure 12 shows clearly that sphingomyelin

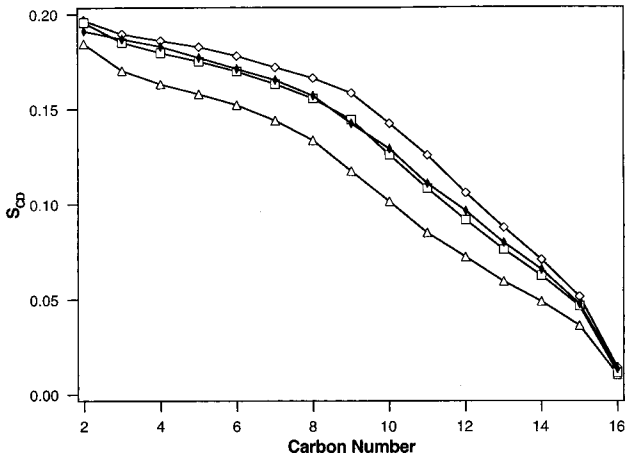

FIGURE 11: Order parameter (S_{CD}) at 37 °C for each carbon on the labeled palmitoyl chain of 31d-PAPC for each of the samples shown in Figure 8, and for pure 31d-PAPC (◆) shown as a comparison: 70% 31d-PAPC/30% SM (◇); 50% 31d-PAPC/30% SM/20% dihydroxyPAPC (□); 80% 31d-PAPC/20% dihydroxyPAPC (△).

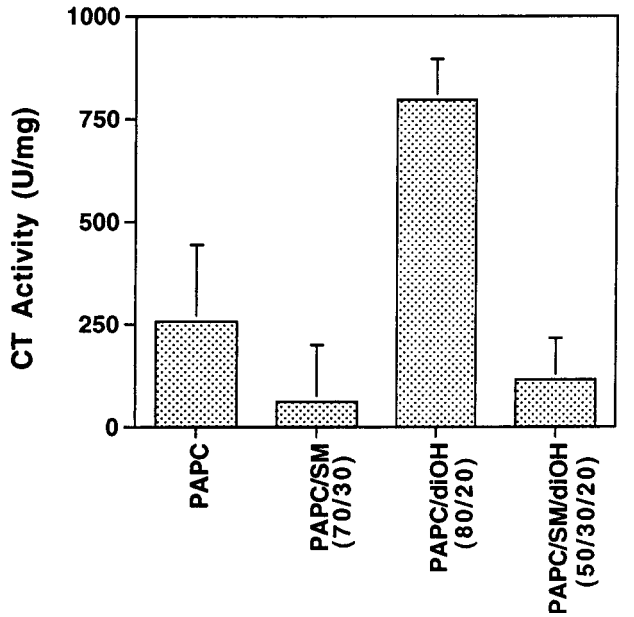

FIGURE 12: Activation of CT by dihydroxyPAPC is reversed by sphingomyelin. The liposomes prepared for ^{2}H NMR were assayed for CT activity as described under Experimental Procedures. Results shown are the average of $n = 8$ for PAPC, and $n = 2$ or 3 for the other lipids. Unpaired *t*-test results for PAPC vs PAPC/SM, PAPC/SM/diOH, and PAPC/diOH are $p = 0.024$, 0.035, and 3.7×10^{-5}, respectively.

inhibits the activation of CT by dihydroxyPAPC. Given the NMR evidence for the reversal by SM of the disordering effect of dihydroxyPC, these data strengthen the correlation between CT activity and bilayer order.

DISCUSSION

The data in this study suggest that the activation of CT by oxidized PC is the result of effects on lipid order. CT can also be activated by free fatty acids and by anionic detergents. The amount of arachidonic acid released during lipoxidase oxidation was approximately 6% of the total mixture of oxidized lipids. Therefore, the maximum amount of free arachidonic acid in the LOX-PAPC samples used to measure ^{2}H NMR spectra and CT activity was 1.5% of total lipid. This amount of free fatty acid is insufficient to activate

CT (*15, 16*). The potential complication of residual deoxycholate and arachidonate in the unpurified LOX-PAPC was eliminated in samples containing the HPLC-purified dihydroxyPAPC. The purified dihydroxyPAPC activated CT as well as the unpurified mixture of oxidized PAPCs (Figures 6 and 9). Thus, the activation of CT was due to the oxidized PAPC rather than the presence of arachidonic acid or deoxycholate in the samples. The changes in molecular order were less for the dihydroxyPAPC compared to LOX-PAPC (Figures 5 and 8). The presence of traces of arachidonic acid and deoxycholate in the latter samples may explain the difference.

CT activity by oxidized PAPCs is also not correlated solely with the large temperature-dependent increases in the central isotropic component observed in the spectra of 31d-PAPC at high mole percent LOX-PAPC (Figure 4). Temperature-dependent increases in isotropic components of deuterium NMR spectra of lipid bilayers have been observed when "budding" eruptions or regions of high curvature in the bilayer surface were present as detected by freeze−fracture electron microscopy (*41*). Wratten et al. (*25*) also observed a temperature-dependent isotropic component in the ESR spectra of lipoxidase-oxidized PL_2PC. We considered the possibility that regions of high curvature in the bilayer, associated with the isotropic component, were responsible for CT activation by LOX-PAPC. Although the isotropic component increased with increasing mole percent of LOX-PAPC, its magnitude varied between preparations of LOX-PAPC, and its contribution to the dihydroxyPAPC spectra was much less than its contribution to the LOX-PAPC spectra. Regardless of the amplitude of the isotropic component in the spectrum, the activation of CT by LOX-PAPC or dihydroxyPAPC was the same for an equivalent mole percent of the oxidized PC. Therefore, CT activation does not correlate with the magnitude of the isotropic component.

Neither does CT activation result from phase separation of components within the bilayer. Phase separation was not observed in the spectra of any of the lipid mixtures used in this study. Thus, the activation of CT is not a result of changes in the relative amounts of inverse hexagonal and lamellar phases, as has been previously observed for protein kinase C activation in bilayers containing diolein (*42*).

The activation of CT by oxidized PC is not due to an interaction of an oxidized PC molecule with a specific binding pocket within CT. CT can be activated by dihydroxyPAPC as shown in the present study, and by hypochlorous acid-oxidized PAPC (*12*), which generates predominantly hypochlorite adducts at double bond positions. Thus, the nature of the polar adduct on the acyl chain is not critical for the activation of CT. Moreover, the activation can be reversed by sphingomyelin, which is chemically distinct from dihydroxyPC and unlikely to compete for a binding pocket.

The parameter that does correlate with CT activation by oxidized PC is reduced acyl chain orientational order. The effect of oxidized phospholipids on membrane order has been studied previously (*25, 26*). Isaacson et al. (*26*) measured ESR order parameters using spin-labeled 1-palmitoyl-2-stearoylPC probes with the doxyl label attached to either C-5 or C-16 of the stearoyl chain. The membrane composition was 30 mol % cholesterol plus 70 mol % phospholipid: PAPC and 15-hydroxyPAPC in various proportions. The magnitudes of the ESR and ^2H NMR molecular order parameters are not expected to agree (*38*), but a comparison of the observed percent reduction in order parameters upon incorporation of oxidized lipids into the membrane is useful. At 38 °C, the spin probe at C-5 reported only small changes in order parameter: increasing the 15-hydroxyPAPC concentration from 3.5% to 14% gave rise to a 2% reduction. The C-16 probe, on the other hand, reported a 13% reduction in the order parameter under the same conditions. These changes are nearly identical to the reductions in S_{CD} we observed at C-5 (4%) and C-15 (14%) of 31d-PAPC when the dihydroxyPAPC content was increased from 0 to 12 mol % at 37 °C. Thus, despite differences in membrane lipid composition, the disrupting effect of hydroxylated lipids on membrane order is consistent. Wratten et al. (*25*) determined order parameters by angle-resolved ESR on oriented bilayers for the probe 3-doxyl-5-α-cholestane in PL_2PC with varying mole percent PL_2PC-OOH or PL_2PC-OH. They observed a similar trend of decreased molecular order with increased mole percent oxidized lipid, although the absolute values for the order parameters and the magnitude of the changes were not directly comparable to our measurements.

That a saturated sphingomyelin species reverses *both* the activation of CT and the membrane disordering by dihydroxyPC firmly establishes a correlation between lipid order and CT activity. Addition of sphingomyelin to lipid bilayers has been shown to increase the order parameter (*29*). In our experiments, sphingomyelin increased the order parameters for the PAPC/diOHPAPC mixture to values nearly identical to those for PAPC alone. Similarly, SM reduced CT activation by PAPC/diOHPAPC to values similar to those obtained with PAPC alone.

Oxidation of the arachidonoyl chain in both LOX-PAPC and dihydroxyPAPC decreased the order of all carbons along the adjacent palmitoyl chain, with the greatest changes in order occurring at the ends of the palmitoyl chain (carbons 10−15). Fractional changes in order are always observed to be greatest toward the ends of the chains for membrane-thinning events, such as increasing temperature or reducing cholesterol content (*43*). However a careful comparison of relative changes in order near the lipid backbone and near the end of the chain reveals that the gradient of the fractional change in order parameter along the chain is steeper for oxidized membranes than for heated or cholesterol-depleted membranes. For example, heating a POPC membrane from 50 to 70 °C results in a reduction in order of 11% at C-3 and of 17% at C-14 (*43*). Increasing the incorporation of dihydroxyPAPC from 0 to 18 mol % results in a reduction in order at C-3 of 7% and at C-14 of 23%. Thus, the oxidized PCs tend to disorder the distal more than the proximal portions of the chains compared to the effects of a general membrane fluidizer. These differential effects may be due to a tendency of the polar OH or OOH groups to migrate toward the lipid−water interface (snorkeling), thus creating voids in the deeper regions of the bilayer, which would permit greater mobility at the ends of the palmitoyl chain. Like oxidized PC, short-chain DAGs can cause differential changes in bilayer order in the proximal vs distal regions of the acyl chain as assessed by ^2H NMR (*42*). The distal regions were more disordered in the presence of diC8 DAG due to the creation of voids deep within the bilayer. On the other hand, the proximal regions were more ordered, due to the small headgroup of the DAG, which allows for tighter

bilayer packing near the surface (*42*). Unlike the short-chain DAGs, oxidized PCs induce an expansion in molecular area due to the snorkeling chains (*9*), and this would disorder the chains in both the proximal and distal portions, with the greatest effect on the distal segment. Snorkeling of oxidized chains, leading to increased area per molecule, has been proposed to explain the increased activity of PLA_2 toward oxidized phospholipids at the bilayer surface (*9, 44*). In the case of PLA_2, the decreased packing density may facilitate access of enzyme to the *sn*-2 ester bond. For CT, the decreased packing density at the surface would facilitate the intercalation of the nonpolar face of the CT amphipathic helix into the lipid bilayer (*20, 23, 24, 40*), which is required for the conformational change leading to enzyme activation (*20*). Although we have measured only the activity and not the binding of the enzyme to the lipid vesicles, binding to vesicles and CT activation are coincident (*18*). This and other studies (*17, 23*) suggest that the distortion of lipid packing to facilitate access to the hydrocarbon core of the bilayer is a key feature in membranes that activate CT. In the previous studies suggesting that looser lipid packing activates CT, other parameters such as headgroup size or charge had also been modified, whereas in the present study the phosphocholine headgroup was unchanged. These results provide the most conclusive demonstration of the importance of lipid packing on the membrane activation of CT.

What is the physiological rationale for activation of CT by oxidized PC? CT catalyzes the rate-limiting step in de novo synthesis of PC. The activation by oxidized PCs may provide a rapid pathway for replacing oxidatively damaged membrane phospholipids.

ACKNOWLEDGMENT

We thank Dr. Alan Tracey for help with interpretation of the ^{13}C and ^{1}H NMR spectra, and Ms. Marcy Tracey for technical assistance with the 400 MHz NMR. We thank Mr. Roland Burton for technical assistance with the mass spectrometry. We also thank Drs. Rebecca Arnold and Dallas Veitch for purification of CT, and Dr. Theresa Kitos for help with the purification of dihydroxyPAPC.

REFERENCES

1. Irani, K., Xia, Y., Zweier, J. L., Sollot, S. J., Der, C. J., Fearon, E. R., Sundaresan, M., Finkel, T., and Goldschmidt-Clermont, P. J. (1997) *Science 275*, 1649−1652.
2. Sundaresan, M., Yu, Z.-X., Ferrans, J., Irani, K., and Finkel, T. (1995) *Science 270*, 296−299.
3. Jacobson, M. D. (1996) *Trends Biochem. Sci. 21*, 83−86.
4. Halliwell, B., and Chirico, S. (1993) *Am. J. Clin. Nutr. 57 (Suppl.)*, 715S−724S.
5. Jones, G. D., Russell, L., Darley-Usmar, V. M., Stone, D., and Wilson, M. T. (1996) *Biochemistry 35*, 7197−7203.
6. Bielicki, J. K., and Forte, T. M. (1999) *J. Lipid Res. 40*, 948−954.
7. Davit-Spraul, A., Therond, P., Leroy, A., Palmade-Rieunier, F., Rousset, C., Moatti, N., and Legrand, A. (1999) *FEBS Lett. 447*, 106−110.
8. Rashha-Step, J., Tatoyan, A., Duncan, R., Ann, D., Pushpa-Rehka, T. R., and Sevanian, A. (1997) *Arch. Biochem. Biophys. 343*, 44−54.
9. van den Berg, J. J. M., Op den Kamp, J. A. F., Lubin, B. H., and Kuypers, F. A. (1993) *Biochemistry 32*, 4962−4967.
10. Natarajan, V., Scribner, W. M., Hart, C. M., and Parthasarathy, S. (1995) *J. Lipid Res. 36*, 2005−2016.
11. Claus, R., Fyrnys, B., Deigner, H. P., and Wolf, G. (1996) *Biochemistry 35*, 4911−4922.
12. Drobnies, A. E., Venczel, E. A., and Cornell, R. B. (1998) *Biochim. Biophys. Acta 1393*, 90−98.
13. Johnson, J. E., and Cornell, R. B. (1999) *Mol. Membr. Biol. 16*, 217−235.
14. Feldman, D. A., Kovac, C. R., Dranginis, P. L., and Weinhold, P. A. (1978) *J. Biol. Chem. 253*, 4980−4986.
15. Feldman, D. A., and Weinhold, P. A. (1987) *J. Biol. Chem. 262*, 9075−9081.
16. Johnson, J. E., Kalmar, G. B., Sohal, P. S., Walkey, C. J., Yamashita, S., and Cornell, R. B. (1992) *Biochem. J. 285*, 815−820.
17. Cornell, R. B. (1991b) *Biochemistry 30*, 5881−5888.
18. Arnold, R. S., DePaoli-Roach, A. A., and Cornell, R. B. (1997) *Biochemistry 36*, 6149−6156.
19. Jamil, H., Hatch, G. M., and Vance, D. E. (1993) *Biochem. J. 291*, 419−427.
20. Arnold, R. S., and Cornell, R. B. (1996) *Biochemistry 35*, 9917−9924.
21. Sleight, R. G., and Dao, H. N. (1990) *Lipids 25*, 100−107.
22. Attard, G. S., Smith, W. S., Templer, R. H., Hunt, A. N., and Jackowski, S. (1998) *Biochem. Soc. Trans. 26*, S230.
23. Johnson, J. E., Aebersold, R., Drobnies, A., and Cornell, R. B. (1997) *Biochim. Biophys. Acta 1324*, 273−284.
24. Johnson, J. E., Rao, N. M., Hui, S.-W., and Cornell, R. B. (1998) *Biochemistry 37*, 9509−9519.
25. Wratten, M. L., van Ginkel, G., van't Veld, A. A., Bekker, A., van Faassen, E. E., and Sevanian, A. (1992) *Biochemistry 31*, 10901−10907.
26. Isaacson, Y., Sherbourne, C. D., Gross, R. W., and Stenson, W. F. (1990) *Chem. Phys. Lipids 52*, 217−226.
27. Eskola, J., and Laakso, S. (1983) *Biochim. Biophys. Acta 751*, 305−311.
28. Brash, A. R., Ingram, C. D., and Harris, T. M. (1987) *Biochemistry 26*, 5465−5471.
29. Holopainen, J. M., Subramanian, M., and Kinnunen, P. K. J (1998) *Biochemistry 37*, 17562−17570.
30. Bartlett, G. R. (1959) *J. Biol. Chem. 234*, 466−468.
31. Bligh, E. G., and Dyer, W. J. (1959) *Can. J. Physiol. 57*, 911−917.
32. Recknagel, R. O., and Glende, E. A., Jr. (1984) *Methods Enzymol. 105*, 331−337.
33. Braun, S., Kalinowski, H.-O., and Berger, S. (1996) *100 and more Basic NMR Experiments*, VCH Publishers, New York.
34. Davis, J. H., Jeffrey, K. R., Bloom, M., Valic, M. I., and Higgs, T. P. (1976) *Chem. Phys. Lett. 42*, 390−394.
35. Davis, J. H. (1979) *Biophys. J. 27*, 339−358.
36. Sternin, E. (1985) *Rev. Sci. Instrum. 56*, 2043−2049.
37. Sternin, E., Bloom, M., and MacKay, A. L. (1983) *J. Magn. Reson. 55*, 274−282.
38. Lafleur, M., Fine, B., Sternin, E., Cullis, P. R., and Bloom, M. (1989) *Biophys. J. 56*, 1037−1041.
39. Seelig, J. (1977) *Q. Rev. Biophys. 10*, 353−418.
40. Johnson, J. E., and Cornell, R. B. (1994) *Biochemistry 33*, 4327−4335.
41. Nezil, F. A., Bayerl, S., and Bloom, M. (1992) *Biophys. J. 61*, 1413−1426.
42. Goldberg, E. M., and Zidovetski, R. (1998) *Biochemistry 37*, 5623−5632.
43. Lafleur, M., Cullis, P. R., and Bloom, M. (1990) *Eur. Biophys. J. 19*, 55−62.
44. van Kuijk, F. J. G. M., Sevanian, A., Handelman, G. J., and Dratz, E. A. (1987) *Trends Biochem. Sci. 12*, 31−34.

BI991573V